

Spin-isospin excitation of ^3He with three-proton final state

Souichi Ishikawa

*Science Research Center, Hosei University, 2-17-1 Fujimi, Chiyoda, Tokyo
102-8160, Japan*

**E-mail: ishikawa@hosei.ac.jp*

.....
Spin-isospin excitation of ^3He nucleus by proton-induced charge-exchange reaction, $^3\text{He}(p,n)ppp$, at forward neutron scattering angle is studied in a plane wave impulse approximation (PWIA). In PWIA, cross sections of the reaction is written in terms of proton-neutron scattering amplitudes and response functions of the transition from ^3He to three-proton state by spin-isospin transition operators. The response functions are calculated with realistic nucleon-nucleon potential models using a Faddeev three-body method. Calculated cross sections agree with available experimental data in substance. Possible effects arising from the uncertainty of proton-neutron amplitudes and three-nucleon interactions in three-proton system are examined.
.....

Subject Index D00, D05, D22

1 Introduction

Three-nucleon (3N) systems: ${}^3\text{H}$, ${}^3\text{He}$, nucleon-deuteron elastic and breakup reactions, etc., have been playing important roles in the quest for the details of interactions among nucleons. These systems are essentially total isospin $T = \frac{1}{2}$ states. (Although the breaking of charge symmetry in nuclear interaction and the Coulomb interaction allow a mixture of $T = \frac{3}{2}$ components, its percentage is quite small [1].) On the other hand, knowledge of interactions among three nucleons, especially of three-nucleon interactions, in $T = \frac{3}{2}$ states is expected for studies on heavier nuclei, neutron-rich nuclei, neutron-star matter, etc. Since there is no bound state of three-neutron ($3n$) and three-proton ($3p$) systems, which are typical $T = \frac{3}{2}$ states [2], observables related these systems may be obtained from nuclear reactions that produce them as final continuum states. Reaction mechanism of such reaction needs to be simple as possible to reduce ambiguity in extracting information on the nuclear interaction.

In the present paper, I will study a charge-exchange reaction: ${}^3\text{He}(p, n)ppp$ reaction at incident proton energies of several hundreds MeV and the reaction angle $\theta_n = 0^\circ$. Although this is a four-body reaction that is still difficult to perform rigorous calculations at high energies, the cross section of the reaction in PWIA is written in terms of $n(p, n)p$ (pn) scattering amplitudes and response functions of 3N system. The former can be taken from nucleon-nucleon (NN) databases [3, 4]. The latter corresponds to a transition from the initial ${}^3\text{He}$ bound state to final $3p$ continuum states, in which one needs to solve three-body problem.

The present author has developed a method to solve the quantum mechanical three-body problem applying the Faddeev method [5]. This method is based on solving the Faddeev equation as integral equations in coordinate space, which even includes long range Coulomb force effects [6, 7], and has been successfully applied for the proton-deuteron systems [8] and three alpha-particles systems [9]. In this paper, this method will be applied for calculating the response functions of $3p$ final states.

In Ref. [10], the cross section $I(0^\circ)$ for the ${}^3\text{He}(p, n)ppp$ reaction at the incident proton energy $T_p = 200$ MeV was measured. In Ref. [11], the polarization transfer coefficient in the transverse direction, $D_{NN}(0^\circ)$, and that in the longitudinal direction, $D_{LL}(0^\circ)$, as well as $I(0^\circ)$ were measured at $T_p = 346$ MeV. One of the measured polarization transfer coefficients, $D_{NN}(0^\circ)$, is consistent with the corresponding pn values. However, the other one, $D_{LL}(0^\circ)$, deviates from the pn values. The authors of Ref. [11] show that this discrepancy may be attributed to a $3p$ resonance with spin-parity $\frac{1}{2}^-$.

Existence of resonant states in multi-neutron or multi-proton states has been a long-standing problem in nuclear physics. Recent compilation of the mass number $A = 3$ systems

[2] reports negatively for the existing of $A = 3$ resonance. In Ref. [12], a possibility of existing of four-neutron (tetra-neutron, $4n$) resonant state was reported. In Ref. [13], it was shown that the existing of the $4n$ resonant state demands an attractive $T = \frac{3}{2}$ three-nucleon potential (3NP) that is tremendously strong. Effects of such a 3NP on the $3p$ system will be studied.

In Sec. 2, I will summarize the formalisms to calculate the response functions and then observables in ${}^3\text{He}(p, n)ppp$ ($\theta_n = 0^\circ$) reaction. In Sec. 3, I will show some results of calculations and compare them with available experimental data. Summary will be given in Sec. 4. In appendix, some kinematical values related to the reaction will be summarized.

2 Theoretical background

In this section, I will consider the charge-exchange reaction, ${}^3\text{He}(\vec{p}, \vec{n})ppp$ ($\theta_n = 0^\circ$) by PWIA, in which the $n(\vec{p}, \vec{n})p$ ($\theta_n = 0^\circ$) scattering amplitude and response functions for the transition from ${}^3\text{He}$ to $3p$ continuum states are the basic elements. (See Refs. [14, 15], e.g., for the general formalism of PWIA.) Kinematics of the reaction is characterized by the incident proton energy in the laboratory (Lab.) system T_p , and the energy transfer in Lab. system ω_{Lab} defined by Eq. (A2a) in Appendix. The direction of the incident proton and thus of the outgoing neutron is taken to be z -axis.

First, I introduce the $3p$ Hamiltonian in the center of mass (c.m.) system,

$$\hat{H}_{3p} = \hat{H}_0 + \hat{V}, \quad (1)$$

where \hat{H}_0 is the kinetic energy operator of the three-body system, and \hat{V} is an interaction potential, which consists of two-nucleon potentials (2NPs) and 3NPs.

Let $|\Psi_{m_1 m_2 m_3}^{(\pm)}(\mathbf{q}, \mathbf{p})\rangle$ be an eigenstate of the Hamiltonian \hat{H}_{3p} associated with an asymptotic $3p$ -state, in which the relative momentum between two protons is \mathbf{q} , the momentum of the third proton with respect to c.m. of the proton-pair is \mathbf{p} , and the spin projection of the proton i is m_i . The superscript (\pm) expresses the outgoing (+) or incoming (−) boundary condition.

The eigenvalue problems is written as

$$\hat{H}_{3p}|\Psi_{m_1 m_2 m_3}^{(\pm)}(\mathbf{q}, \mathbf{p})\rangle = E(\mathbf{q}, \mathbf{p})|\Psi_{m_1 m_2 m_3}^{(\pm)}(\mathbf{q}, \mathbf{p})\rangle, \quad (2)$$

with

$$E(\mathbf{q}, \mathbf{p}) = \frac{q^2}{m_p} + \frac{3p^2}{4m_p}, \quad (3)$$

where m_p is the mass of the proton.

A response function corresponding to the transition from the ^3He state with spin projection M , $|\Psi_M\rangle$, to $3p$ -continuum states with energy E by an operator \hat{O} is given by

$$R(E) = \frac{1}{2} \sum_{M=\pm\frac{1}{2}} \sum_{m_1, m_2, m_3} \int d\mathbf{q} d\mathbf{p} |T(\mathbf{q}, \mathbf{p}, m_1, m_2, m_3, M)|^2 \delta(E - E(\mathbf{q}, \mathbf{p})), \quad (4)$$

where E is related to kinematical values of the reaction as Eq. (A9), and the transition amplitude is defined by

$$T(\mathbf{q}, \mathbf{p}, m_1, m_2, m_3, M) = \langle \Psi_{m_1 m_2 m_3}^{(-)}(\mathbf{q}, \mathbf{p}) | \hat{O} | \Psi_M \rangle. \quad (5)$$

Using the completeness of the $3p$ states, we have

$$\begin{aligned} R(E) &= \frac{1}{2} \sum_{M=\pm\frac{1}{2}} \langle \Psi_M | \hat{O}^\dagger \delta(E - \hat{H}_{3p}) \hat{O} | \Psi_M \rangle \\ &= -\frac{1}{2\pi} \sum_{M=\pm\frac{1}{2}} \text{Im} \langle \Psi_M | \hat{O}^\dagger \frac{1}{E + i\epsilon - \hat{H}_{3p}} \hat{O} | \Psi_M \rangle. \end{aligned} \quad (6)$$

Here, I introduce a wave function $|\Xi_M\rangle$ describing the disintegration process [16],

$$|\Xi_M\rangle = \frac{1}{E + i\epsilon - \hat{H}_{3p}} \hat{O} | \Psi_M \rangle, \quad (7)$$

from which the transition amplitude is calculated as follows:

$$T(\mathbf{q}, \mathbf{p}, m_1, m_2, m_3, M) = \langle \Phi_{m_1, m_2, m_3}^{3p}(\mathbf{q}, \mathbf{p}) | \hat{O} | \Psi_M \rangle + \langle \Phi_{m_1, m_2, m_3}^{3p}(\mathbf{q}, \mathbf{p}) | \hat{V} | \Xi_M \rangle, \quad (8)$$

where $|\Phi_{m_1, m_2, m_3}^{3p}(\mathbf{q}, \mathbf{p})\rangle$ is the initial state corresponding to $|\Psi_{m_1, m_2, m_3}^{(+)}(\mathbf{q}, \mathbf{p})\rangle$.

Numerical solution of Eq. (7) is obtained by the method based on the Faddeev three-body theory [5], whose formal and technical details are essentially same as those used for the proton-deuteron scattering [7, 8] and three alpha-particles [9] problems.

The $n(\vec{p}, \vec{n})p$ ($\theta_n = 0^\circ$) amplitude consists of three independent terms:

$$f_{pn} = \mathcal{V}_c + \mathcal{V}_L (\boldsymbol{\sigma}_p \cdot \hat{\mathbf{z}}) (\boldsymbol{\sigma}_n \cdot \hat{\mathbf{z}}) + \mathcal{V}_T (\boldsymbol{\sigma}_p \times \hat{\mathbf{z}}) \cdot (\boldsymbol{\sigma}_n \times \hat{\mathbf{z}}), \quad (9)$$

where $\boldsymbol{\sigma}_p$ ($\boldsymbol{\sigma}_n$) is the Pauli spin matrix of the incident proton (the outgoing neutron); \mathcal{V}_c , \mathcal{V}_L , and \mathcal{V}_T , are spin-scalar, spin-longitudinal, and spin-transverse components of the amplitude, respectively.

The pn observables, differential cross section, polarization transfer coefficients, are given as follows:

$$\sigma^{pn}(0^\circ) = |\mathcal{V}_c|^2 + |\mathcal{V}_L|^2 + 2|\mathcal{V}_T|^2, \quad (10a)$$

$$D_{LL}^{pn}(0^\circ) = \frac{|\mathcal{V}_c|^2 + |\mathcal{V}_L|^2 - 2|\mathcal{V}_T|^2}{|\mathcal{V}_c|^2 + |\mathcal{V}_L|^2 + 2|\mathcal{V}_T|^2}, \quad (10b)$$

$$D_{NN}^{pn}(0^\circ) = \frac{|\mathcal{V}_c|^2 - |\mathcal{V}_L|^2}{|\mathcal{V}_c|^2 + |\mathcal{V}_L|^2 + 2|\mathcal{V}_T|^2}. \quad (10c)$$

In the process considered, there are three operators corresponding to each term of Eq. (9): the isovector spin-scalar operator \hat{O}_c , the isovector spin-longitudinal operator \hat{O}_L , and the isovector spin-transverse operator \hat{O}_T , which are defined by

$$\hat{O}_c = \sum_{i=1}^3 e^{iQ_{c.m.}\hat{\mathbf{z}}\cdot\mathbf{r}_i} t_i^{(+)}, \quad (11a)$$

$$\hat{O}_L = \sum_{i=1}^3 e^{iQ_{c.m.}\hat{\mathbf{z}}\cdot\mathbf{r}_i} (\hat{\mathbf{z}} \cdot \boldsymbol{\sigma}_i) t_i^{(+)}, \quad (11b)$$

$$\hat{O}_T = \sum_{i=1}^3 e^{iQ_{c.m.}\hat{\mathbf{z}}\cdot\mathbf{r}_i} (\hat{\mathbf{z}} \times \boldsymbol{\sigma}_i) t_i^{(+)}, \quad (11c)$$

where $Q_{c.m.}$ is the momentum transfer, Eq. (A8b) in Appendix, $t_i^{(+)}$ an isospin operator that transforms the neutron i in ^3He to proton i in the final $3p$ state, \mathbf{r}_i ($\boldsymbol{\sigma}_i$) the coordinate vector in the $3N$ -c.m. system (the Pauli spin matrix) of the particle i . The corresponding response functions will be denoted as $R_c(E)$, $R_L(E)$, and $R_T(E)$, respectively,

The unpolarized differential cross section $I(0^\circ)$ and the polarization transfer coefficients, $D_{LL}(0^\circ)$ and $D_{NN}(0^\circ)$, for the $^3\text{He}(p, n)ppp$ ($\theta_n = 0^\circ$) reaction are expressed as

$$I(0^\circ) = N_K \left(|\mathcal{V}_c|^2 R_c + |\mathcal{V}_L|^2 R_L + 2|\mathcal{V}_T|^2 R_T \right), \quad (12a)$$

$$D_{LL}(0^\circ) = \frac{|\mathcal{V}_c|^2 R_c + |\mathcal{V}_L|^2 R_L - 2|\mathcal{V}_T|^2 R_T}{|\mathcal{V}_c|^2 R_c + |\mathcal{V}_L|^2 R_L + 2|\mathcal{V}_T|^2 R_T}, \quad (12b)$$

$$D_{NN}(0^\circ) = \frac{|\mathcal{V}_c|^2 R_c - |\mathcal{V}_L|^2 R_L}{|\mathcal{V}_c|^2 R_c + |\mathcal{V}_L|^2 R_L + 2|\mathcal{V}_T|^2 R_T}, \quad (12c)$$

where a kinematical factor N_K is given in Eq. (A10) in Appendix.

3 Results and discussion

In this section, calculations of the observables for the reactions, ${}^3\text{He}(p, n)ppp$ ($\theta_n = 0^\circ$), at $T_p = 346$ MeV and 200 MeV will be presented and compared with available experimental data.

Calculations are performed as follows: the three-body equation, Eq. (7), is solved for each of the transition operators, Eqs. (11a) - (11c), from which the transition amplitude, Eq. (5), is calculated by Eq. (8). Then the response functions are calculated from Eq. (4). Using the response functions together with the pn amplitudes in Eq. (9), the observables are calculated by Eqs. (10a) - (10c).

In solving three-body equations, 3N partial wave states for which 2NPs and 3NPs are active, are restricted to those with total NN angular momenta $J \leq 6$ for bound state calculations, and $J \leq 4$ for continuum state calculations. For continuum state calculations, 3N states with total angular momenta $J_0 = \frac{1}{2}$ and $\frac{3}{2}$ are taken into account. An error of these truncating procedures is estimated to be at most 2 % from comparisons of results with $J \leq 4$ NN states and those with $J \leq 3$ ones, and contributions from $J_0 = \frac{5}{2}$ states, which demonstrates that it is good enough for the purposes of the present work.

As realistic models of 2NP, the Argonne V₁₈ model (AV18) [17] and its V₈ version (AV8') [18], the Argonne V₁₄ model (AV14) [19], and a super-soft core model (dTRS) [20] are used. The NN scattering length parameters of these models for ${}^1\text{S}_0$ states: pp , nn , and pn , are compared with empirical values [21] in Table 1. As this table shows, AV8', AV14, and dTRS models are charge independent. In this work, charge-dependent version of AV14 and dTRS in Table 1 are introduced by adding potentials that break the charge independence as done in Ref. [22]. Such potentials for AV14 and dTRS are denoted by AV14(CD) and dTRS(CD), respectively.

The ${}^3\text{He}$ wave function is calculated using each 2NP model with the Brazil model of the two-pion exchange three-nucleon potential given in Ref. [23], whose cutoff mass parameter of the πNN -vertex Λ_π is tuned to reproduce the empirical binding energy [8]. The values of Λ_π in the unit of MeV are 660, 610, 670, and 650 for AV18, AV8', AV14(CD), and dTRS(CD), respectively. It is noted that the ${}^3\text{He}$ wave function by the CD version of AV14 (dTRS) is used for calculations of the original version of AV14 (dTRS).

The $n(\vec{p}, \vec{n})p$ ($\theta_n = 0^\circ$) scattering amplitudes in Eq. (9), \mathcal{V}_c , \mathcal{V}_L , and \mathcal{V}_T , are calculated by Eqs. (10a) - (10c) with the pn observables, $\sigma^{pn}(0^\circ)$, $D_{LL}^{pn}(0^\circ)$, and $D_{NN}^{pn}(0^\circ)$, taken from the SP07 solution [3, 24], which are shown in Table 2.

In Fig. 1, calculated differential cross section $I(0^\circ)$ and polarization transfer coefficients, $D_{NN}(0^\circ)$ and $D_{LL}(0^\circ)$, for the ${}^3\text{He}(p, n)ppp$ reaction at $T_p = 346$ MeV as functions of ω_{Lab} ,

Table 1 Empirical and calculated values for the NN scattering length parameters of 1S_0 - pp , nn , and pn states. For pp system, the scattering length after subtracting the effect of Coulomb force is used. Experimental values are taken from Ref. [21].

	a_{pp}^N (fm)	a_{nn} (fm)	a_{pn} (fm)
Empirical	-17.3 ± 0.4	-18.9 ± 0.4	-23.740 ± 0.020
AV18	-16.6	-18.3	-23.7
AV8'	-19.3	-19.3	-19.3
AV14	-23.7	-23.7	-23.7
AV14 (CD)	-17.7	-18.9	-23.7
dTRS	-18.0	-18.0	-18.0
dTRS (CD)	-16.6	-18.0	-24.1

Table 2 Observables and scattering amplitudes in $n(\vec{p}, \vec{n})p$ reaction at forward angle $\theta_n = 0^\circ$ taken from the SP07 solution [3, 24]. Those used for the calculations of $^3\text{He}(p, n)ppp$ reaction at $T_p = 200$ MeV and 346 MeV are shown.

	$T_p = 200$ MeV	$T_p = 346$ MeV
$\sigma^{pn}(0^\circ)$ [mb/sr]	12.47	11.32
$D_{LL}^{pn}(0^\circ)$	-0.1831	-0.3942
$D_{NN}^{pn}(0^\circ)$	-0.3269	-0.2396
$ \mathcal{V}_c ^2$ [mb/sr]	0.5085	0.3583
$ \mathcal{V}_L ^2$ [mb/sr]	4.5849	3.0705
$ \mathcal{V}_T ^2$ [mb/sr]	3.6883	3.9456

are compared with the experimental data of Ref. [11]. In Fig. 2, calculated values of $I(0^\circ)$ for $T_p = 200$ MeV are compared with the experimental data [10]. In both figures, calculations of all 2NP models in Table 2 fall within narrow bands, which demonstrates small pp -2NP dependency of the observables.

The calculations of $I(0^\circ)$ at $T_p = 346$ MeV reproduce the data well except some deviations around $\omega_{Lab} = 20$ MeV. Those at $T_p = 200$ MeV reproduce the lineshape of the data with a reduction by about 30%.

The calculated and experimental values of $D_{NN}(0^\circ)$ and calculated $D_{LL}(0^\circ)$ are almost consistent with the pn values, which are expressed by the dashed horizontal lines in Figs. 1 (b) and (c). On the other hand, the experimental values of $D_{LL}(0^\circ)$ deviate from the pn values with an energy-transfer dependence, from which the authors of Ref. [11] predicted

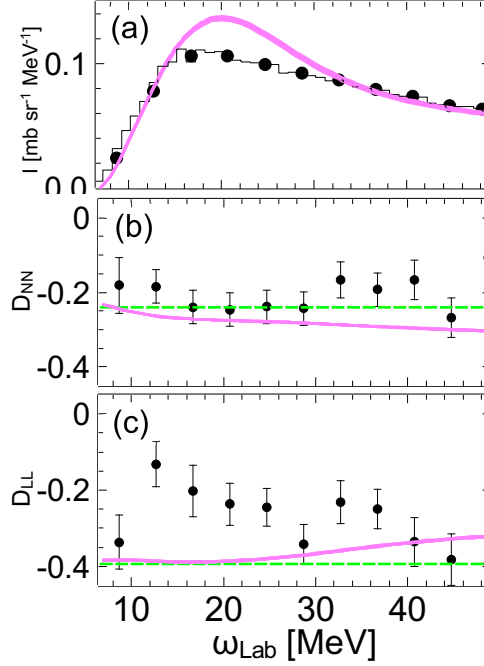


Fig. 1 Differential cross section $I(0^\circ)$ (a) and polarization transfer coefficients, $D_{NN}(0^\circ)$ (b) and $D_{LL}(0^\circ)$ (c), for the ${}^3\text{He}(p, n)ppp$ reaction at $T_p = 346$ MeV. Calculations with all 2NP models in Table 1 are shown by bands (light magenta). The experimental data (black points and histogram) are taken from Ref. [11]. Dashed horizontal lines (green) in (b) and (c) are the corresponding pn values in Table 2.

the existence of a $3p$ resonance in $\frac{1}{2}^-$ state centered at $\omega_r = 16 \pm 1$ MeV with the width of $\Gamma = 11 \pm 3$ MeV.

Using three observables measured in Ref. [11] along with the pn amplitudes in Table 2, the response functions, R_c , R_L , and R_T , are calculated by Eqs. (12a) - (12c). Thus obtained response functions are compared with the calculated ones with AV18 in Fig. 3. The figure shows that the extracted R_L and R_T have similar shape and magnitude as the calculations, but the extracted R_c is a few times larger than the calculation. The resonance-like behavior in $D_{LL}(0^\circ)$ as a function of ω_{Lab} is reflected in R_c , but not in R_L and R_T . However, the calculations are not able to reproduce this tendency.

The observables in this work largely owe to the pn amplitudes, which are related pn observables as Eqs. (10a)-(10c). Since there is few experimental data of corresponding pn observables [25], the uncertainty in the pn amplitudes used in this work is not small. Thus, I have evaluated the pn amplitudes inversely from the calculated response functions, R_c , R_L , and R_T , and the experimental data of $I(0^\circ)$, $D_{NN}(0^\circ)$, and $D_{LL}(0^\circ)$ by Eqs. (12a) - (12c).

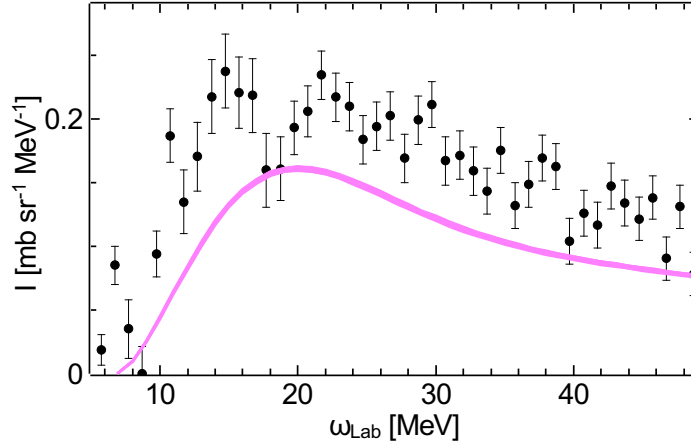


Fig. 2 Differential cross section $I(0^\circ)$ for the ${}^3\text{He}(p, n)ppp$ reaction at $T_p = 200$ MeV. Calculations with all 2NP models in Table 1 are shown by band (light magenta). The experimental data are taken from Ref. [10].

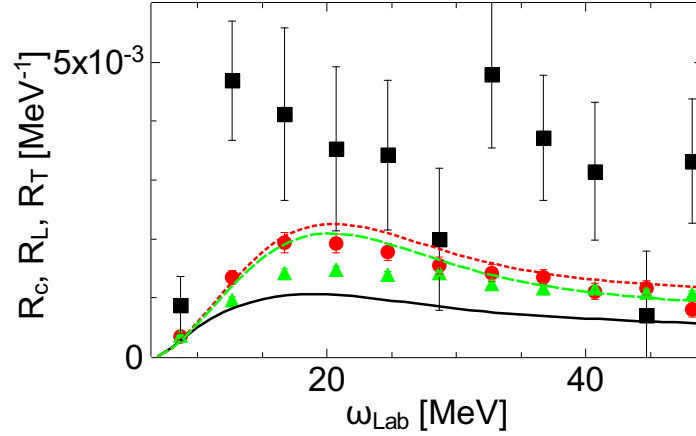


Fig. 3 Data points with error bars are the response functions R_c (black squares), R_L (red circles), and R_T (green triangles), extracted from the data [11] and the pn amplitudes from the SP07 solution. Curves are calculated response functions with AV18 for R_c (black solid line), R_L (red dotted line), and R_T (green dashed line).

The pn -amplitudes obtained in this way depend on ω_{Lab} that the experimental data exist. Taking the average, one obtains: $|\mathcal{V}_c|^2 = 1.43 \pm 0.57$ mb/sr, $|\mathcal{V}_L|^2 = 2.90 \pm 0.38$ mb/sr, and $|\mathcal{V}_T|^2 = 3.60 \pm 0.75$ mb/sr, from which the pn observables are calculated as: $\sigma^{pn}(0^\circ) = 11.5 \pm 1.7$ mb/sr, $D_{LL}^{pn}(0^\circ) = -0.24 \pm 0.11$, and $D_{TT}^{pn}(0^\circ) = -0.13 \pm 0.05$. The errors are only

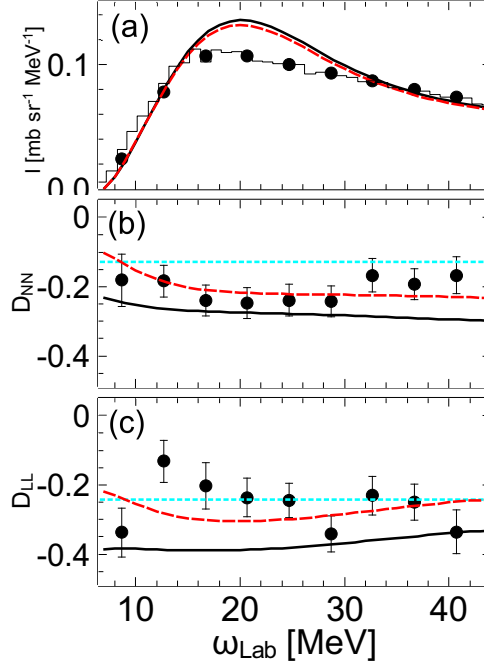


Fig. 4 Same as Fig. 1. Calculations for AV18 with the pn amplitudes taken from the SP07 solution are shown by sold (black) lines. Those with the fitted pn amplitudes (see the text) are shown by the dashed (red) lines. Dotted horizontal lines (cyan) in (b) and (c) are the pn values calculated with the fitted pn amplitudes.

statistical ones with respect to the averaging procedure, and effects of the experimental error are not taken into account.

Fig. 4 shows the calculated observables with the above fitted pn -amplitudes (only the central values are used.), which gives a better agreement with the data, although the rapid dependence of $D_{LL}(0^\circ)$ is not reproduced.

Next, I will study effects of 3NP on the observables. Recently, the possibility of a resonant $4n$ state at low energy is indicated experimentally in Ref. [12]. In Ref. [13], effects of $T = \frac{3}{2}$ 3NP on $4n$ -system as well as $3n$ -system are studied. The functional form of 3NP used in Ref. [13] is as follows.

$$V^{3NP}(T) = \sum_{n=1}^2 W_n(T) e^{-(r_{ij}^2 + r_{jk}^2 + r_{ki}^2)/b_n^2} \mathcal{P}_{ijk}(T), \quad (13)$$

where $T = \frac{1}{2}$ or $\frac{3}{2}$, r_{ij} is the distance between the i -th and j -th nucleons, and $\mathcal{P}_{ijk}(T)$ is a projection operator on the 3N isospin T state.

The range parameters used in Refs. [13, 26] are $b_1 = 4.0$ fm and $b_2 = 0.75$ fm. The strength parameters of the shorter range term $W_2(T)$ for both of $T = \frac{1}{2}$ and $T = \frac{3}{2}$ are fixed to be

35.0 MeV in Ref. [13], and also in this work. The required value of the strength parameter for the longer range term $W_1(\frac{3}{2})$ for $J^\pi = 0^+$ $4n$ -state to bind as the lower bound of the experimental value [12] is -36.14 MeV [13]. This value contrasts with $W_1(\frac{1}{2}) = -2.04$ MeV, which is determined to reproduce the binding energies of ^3H , ^3He , and ^4He in combination with Argonne V_8' (AV8') NN potential [18].

In the following, I will use the AV18, which is more repulsive than AV8' in $3\text{N}(T = \frac{1}{2})$ bound state. As a consequence of this, a more attractive value: $W_1(\frac{1}{2}) = -2.55$ MeV, is used to reproduce ^3He binding energy. However, this difference may not be essential in the present case.

In Fig. 5, calculated values with $V^{3\text{NP}}(\frac{3}{2})$ taking $W_1(\frac{3}{2}) = -36.0$ MeV are compared with the AV18 calculations. The introduction of the $V^{3\text{NP}}(\frac{3}{2})$ shifts the peak of the cross section to higher in the magnitude and lower in the position, which makes the agreement with the experimental data worse than the AV18 calculation. On the other hand, effects of the 3NP on the $D_{NN}(0^\circ)$ and $D_{LL}(0^\circ)$ are quite small. These rather small effects of the 3NP on the $3p$ system in spite of the large value of $W_1(\frac{3}{2})$ are however consistent with the analysis of $3n$ systems in Ref. [13], and should be due to a large separation among three protons by the Pauli principle.

In Ref. [13], dependence of the strength parameters in the 3NP on the total angular momentum and parity J_0^π is not considered for simplicity. Here, I will examine the J_0^π -dependence of the parameter $W_1(\frac{3}{2})$. In Table 3, results of $D_{LL}(0^\circ)$ calculated including $V^{3\text{NP}}(\frac{3}{2})$ with $W_1(\frac{3}{2}) = -36.0$ MeV for all four states: $J_0^\pi = \frac{1}{2}^\pm$ and $\frac{3}{2}^\pm$, or for only one partial wave state, are shown. Even though the effects are not so large compared to the difference between the data and AV18 calculation, it looks that only $V^{3\text{NP}}(\frac{3}{2})$ with $J_0^\pi = \frac{1}{2}^-$ is effective to the difference.

Fig. 6 shows the observables calculated with $V^{3\text{NP}}(\frac{3}{2})$ that is effective only for $J_0^\pi = \frac{1}{2}^-$ state taking $W_1(\frac{3}{2})$ from -36 MeV to -90 MeV. It looks that the 3NP with $W_1(\frac{3}{2}) = -90$ MeV produces a resonance at $\omega_{Lab} = 9$ MeV with a narrow width (about 2 MeV), which produces some visible effects on $D_{LL}(0^\circ)$ and $D_{NN}(0^\circ)$. The width of the resonance is smaller than the reported in [11].

4 Summary

In this paper, I have presented calculations of the cross section and the polarization transfer coefficients, D_{NN} and D_{LL} , in $^3\text{He}(p, n)ppp$ ($\theta_n = 0^\circ$) reaction with the spin-isospin response functions obtained for some realistic NN potential models.

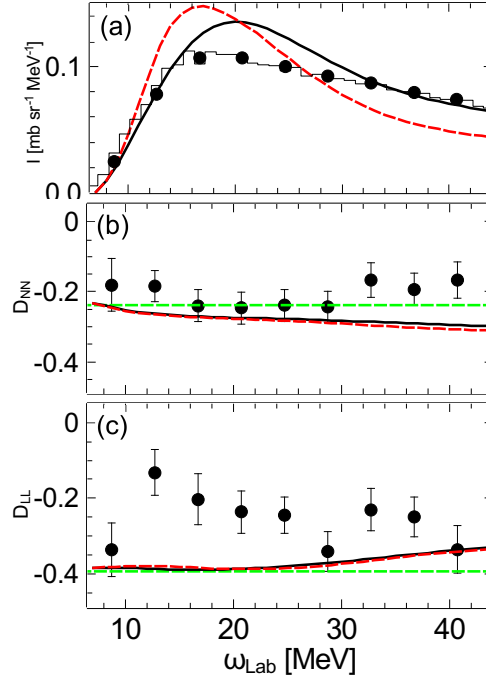


Fig. 5 Same as Fig. 1. Calculations with AV18 are shown by sold (black) lines. Calculations with AV18 plus $V^{3\text{NP}}(\frac{3}{2})$ taking $W_1(\frac{3}{2}) = -36.0$ MeV are shown by dashed (red) lines.

Table 3 Calculated values of the polarization transfer coefficient $D_{LL}(0^\circ)$ for the ${}^3\text{He}(p, n)ppp$ reaction at $T_p = 346$ MeV and at $\omega_{Lab} = 15$ MeV including $V^{3\text{NP}}(\frac{3}{2})$ with $W_1(\frac{3}{2}) = -36.0$ MeV for all four states: $J_0^\pi = \frac{1}{2}^\pm$ and $\frac{3}{2}^\pm$, or for only one partial wave state. $\Delta D_{LL}^{pn}(0^\circ)$ is the difference from the AV18 calculation.

	$D_{LL}^{pn}(0^\circ)$	$\Delta D_{LL}^{pn}(0^\circ)$
AV18	-0.389	
AV18+ $V^{3\text{NP}}(T = \frac{3}{2}) [J_0^\pi = \frac{1}{2}^\pm, \frac{3}{2}^\pm]$	-0.382	0.007
AV18+ $V^{3\text{NP}}(T = \frac{3}{2}) [J_0^\pi = \frac{1}{2}^+]$	-0.391	-0.002
AV18+ $V^{3\text{NP}}(T = \frac{3}{2}) [J_0^\pi = \frac{1}{2}^-]$	-0.379	0.010
AV18+ $V^{3\text{NP}}(T = \frac{3}{2}) [J_0^\pi = \frac{3}{2}^+]$	-0.389	0.000
AV18+ $V^{3\text{NP}}(T = \frac{3}{2}) [J_0^\pi = \frac{3}{2}^-]$	-0.388	0.001

The calculations have little NN potential dependence, and show a reasonable agreement with available experimental data, except that the energy-transfer dependence of $D_{LL}(0^\circ)$ is much smoother than the data.

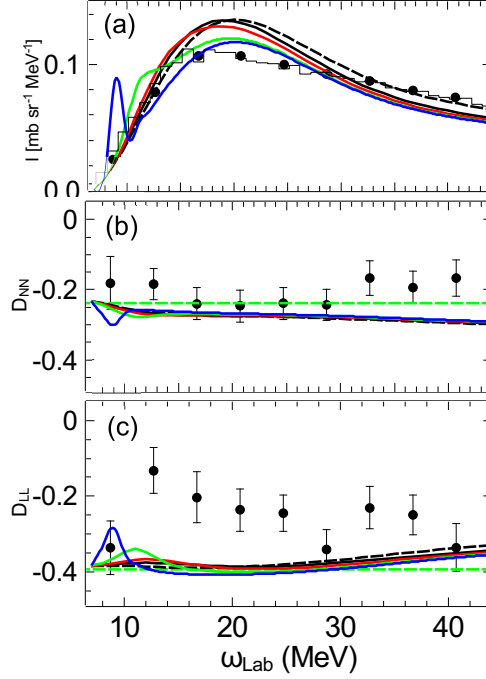


Fig. 6 Same as Fig. 1. Calculations with AV18 are shown by dashed (black) lines. Those with AV18 plus $V^{3\text{NP}}(\frac{3}{2})$ that is active for $J_0^\pi = \frac{1}{2}^-$ state taking $W_1(\frac{3}{2}) = -36, -50, -70$, and -90 MeV, are shown by solid black, red, green, and blue lines, respectively.

Introductions of the attractive 3NP for the $3\text{N}(T = \frac{3}{2})$ state suggested from the analysis of the $4n$ state as well as further strength enhanced 3NPs for $J_0^\pi = \frac{1}{2}^-$ state so as to produce a $3p$ resonance state are examined. But they cannot resolve the discrepancy.

These results suggest that the curious energy-transfer dependence of the experimental $D_{LL}(0^\circ)$, which was the basis of the existence of the $3p$ resonance [11], is not consistent with conventional models of the nuclear interaction, which indicates the need for further experimental studies of the reaction.

Also, a need for good knowledge of observables in $n(\vec{p}, \vec{n})p$ at the very forward angles is stressed to reduce ambiguity in the calculation.

Finally, it is remarked that precise calculations of observables related to $3n$ - or $3p$ -system with theoretical models of the nuclear interactions are now available, which enables us to compare and then to study nuclear interactions whether a 3N resonance does exist or not.

A Kinematics

In this appendix, kinematical values related to ${}^3\text{He}(p, n)ppp$ ($\theta_n = 0^\circ$) reaction are summarized.

Let T_p (T_n) be the incident proton (outgoing neutron) energy in Lab. system. Masses of proton, neutron, and ${}^3\text{He}$ are denoted by m_p , m_n , and $m_{{}^3\text{He}}$, respectively.

- Total energy in Lab. system:

$$E_{tot, Lab} = m_p + T_p + m_{{}^3\text{He}}. \quad (\text{A1})$$

- The energy transfer and momentum transfer in Lab. system:

$$\omega_{Lab} = (m_p + T_p) - (m_n + T_n) \quad (\text{A2a})$$

$$Q_{Lab} = K_p - K_n, \quad (\text{A2b})$$

where

$$K_p = \sqrt{(m_p + T_p)^2 - m_p^2} \quad (\text{A3a})$$

$$K_n = \sqrt{(m_n + T_n)^2 - m_n^2}. \quad (\text{A3b})$$

- Total energy of all four particles in c.m. frame of the initial p - ${}^3\text{He}$ system:

$$E_{tot, c.m.} = \sqrt{E_{tot, Lab}^2 - K_p^2} \quad (\text{A4})$$

- Energy and momentum of the proton and energy of ${}^3\text{He}$:

$$E_{p, c.m.} = \frac{E_{tot, c.m.}^2 + m_p^2 - m_{{}^3\text{He}}^2}{2E_{tot, c.m.}} \quad (\text{A5a})$$

$$k_i = \sqrt{E_{p, c.m.}^2 - m_p^2}. \quad (\text{A5b})$$

$$E_{{}^3\text{He}, c.m.} = E_{tot, c.m.} - E_{p, c.m.} = \frac{E_{tot, c.m.}^2 - m_p^2 + m_{{}^3\text{He}}^2}{2E_{tot, c.m.}} \quad (\text{A5c})$$

- Energies and momentum of the neutron, and energy of $3p$ -system in the c.m. frame of the final n - $3p$ system:

$$E_{n, c.m.} = \frac{E_{tot, c.m.}^2 + m_n^2 - (E_{3p, Lab}^2 - Q_{Lab}^2)}{2E_{tot, c.m.}} \quad (\text{A6a})$$

$$k_f = \sqrt{E_{n, c.m.}^2 - m_n^2}, \quad (\text{A6b})$$

$$E_{3p, c.m.} = E_{tot, c.m.} - E_{n, c.m.} = \frac{E_{tot, c.m.}^2 - m_n^2 + (E_{3p, Lab}^2 - Q_{Lab}^2)}{2E_{tot, c.m.}}, \quad (\text{A6c})$$

where

$$E_{3p, Lab} = m_{{}^3\text{He}} + \omega_{Lab}. \quad (\text{A7})$$

- Energy transfer and momentum transfer in the c.m. system:

$$\omega_{c.m.} = E_{p,c.m.} - E_{n,c.m.} \quad (\text{A8a})$$

$$Q_{c.m.} = k_i - k_f \quad (\text{A8b})$$

- The energy in the c.m. system of the final $3p$:

$$E = \sqrt{E_{3p,c.m.}^2 - k_f^2} - 3m_p. \quad (\text{A9})$$

- The Kinematical factor in the expression, Eq. (12a), is given by

$$N_K = \left(\frac{2\pi}{\hbar}\right)^2 \mu_i \mu_f \frac{k_f}{k_i} \times \left(\frac{K_n}{k_f}\right) \frac{dE}{d\omega_{Lab}}, \quad (\text{A10})$$

where

$$\mu_i = \frac{E_{p,c.m.} E_{3\text{He},c.m.}}{E_{p,c.m.} + E_{3\text{He},c.m.}}, \quad (\text{A11a})$$

$$\mu_f = \frac{E_{n,c.m.} E_{3p,c.m.}}{E_{n,c.m.} + E_{3p,c.m.}}, \quad (\text{A11b})$$

and

$$\frac{dE}{d\omega_{Lab}} = \frac{E_{tot,Lab} - E_{n,Lab} \frac{K_p}{K_n}}{E + 3m_p}. \quad (\text{A12})$$

References

- [1] Y. Wu, S. Ishikawa, and T. Sasakawa, Phys. Rev. Lett. **64**, 1875 (1990); **66**, 242(E) (1991).
- [2] J. E. Purcell, J. H. Kelley, E. Kwan, C. G. Sheu, and H. R. Weller, Nucl. Phys. A **848**, 1 (2010).
- [3] <http://gwdac.phys.gwu.edu/>.
- [4] <http://nn-online.org/>.
- [5] L. D. Faddeev, Zh. Eksp. Teor. Fiz. **39**, 1459 (1961) [Sov. Phys. JETP **12**, 1014 (1961)].
- [6] T. Sasakawa and T. Sawada, Phys. Rev. C **20**, 1954 (1979).
- [7] S. Ishikawa, Few-Body Syst. **32**, 229 (2003).
- [8] S. Ishikawa, Phys. Rev. C **80**, 054002 (2009).
- [9] S. Ishikawa, Phys. Rev. C **87**, 055804 (2013).
- [10] M. Palarczyk, C. M. Riedel, D. Dehnhard, M. A. Espy, M. A. Franey, J. L. Langenbrunner, L. C. Bland, D. S. Carman, B. Brinkmüller, R. Madey, Y. Wang, J. W. Watson, N. S. Chant, Phys. Rev. C **58**, 645 (1998).
- [11] T. Wakasa, E. Ihara, M. Dozono, K. Hatanaka, T. Imamura, M. Kato, S. Kuroita, H. Matsubara, T. Noro, H. Okamura, K. Sagara, Y. Sakemi, K. Sekiguchi, K. Suda, T. Sueta, Y. Tameshige, A. Tamii, H. Tanabe, and Y. Yamada, Phys. Rev. C **77**, 054611 (2008).
- [12] K. Kisamori, S. Shimoura, H. Miya, S. Michimasa, S. Ota, M. Assie, H. Baba, T. Baba, D. Beaumel, M. Dozono, T. Fujii, N. Fukuda, S. Go, F. Hammache, E. Ideguchi, N. Inabe, M. Itoh, D. Kameda, S. Kawase, T. Kawabata, M. Kobayashi, Y. Kondo, T. Kubo, Y. Kubota, M. Kurata-Nishimura, C. S. Lee, Y. Maeda, H. Matsubara, K. Miki, T. Nishi, S. Noji, S. Sakaguchi, H. Sakai, Y. Sasamoto, M. Sasano, H. Sato, Y. Shimizu, A. Stolz, H. Suzuki, M. Takaki, H. Takeda, S. Takeuchi, A. Tamii, L. Tang, H. Tokieda, M. Tsumura, T. Uesaka, K. Yako, Y. Yanagisawa, R. Yokoyama, and K. Yoshida, Phys. Rev. Lett. **116**, 052501 (2016).
- [13] E. Hiyama, R. Lazauskas, J. Carbonell, and M. Kamimura, Phys. Rev. C **93**, 044004 (2016).
- [14] M. Ichimura and K. Kawahigashi, Phys. Rev. C **45**, 1822 (1992); **46**, 2117(E) (1992).
- [15] A. Itabashi, K. Aizawa, and M. Ichimura, Prog. Theor. Phys. **91**, 69 (1994).
- [16] S. Ishikawa, H. Kamada, W. Glöckle, J. Golak, and H. Witała, Phys. Lett. B **339**, 293 (1994).
- [17] R. B. Wiringa, V. G. J. Stoks, and R. Schiavilla, Phys. Rev. C **51**, 38 (1995).

- [18] B. S. Pudliner, V. R. Pandharipande, J. Carlson, S. C. Pieper, and R. B. Wiringa, Phys. Rev. C **56**, 1720 (1997).
- [19] R. B. Wiringa, R. A. Smith, and T. L. Ainsworth, Phys. Rev. C **56**, 1207 (1984).
- [20] R. de Tourreil, B. Rouben, D. W. L. Sprung, Nucl. Phys. A **242**, 445 (1975).
- [21] R. Machleidt and I. Slaus, J. Phys. G **27**, R69 (2001).
- [22] Y. Wu, S. Ishikawa, and T. Sasakawa, Few-Body Syst. **15**, 145 (1993).
- [23] S. Ishikawa and M. R. Robilotta, Phys. Rev. C **76**, 014006 (2007).
- [24] R. A. Arndt, W. J. Briscoe, I. I. Strakovsky, and R. L. Workman, Phys. Rev. C **76**, 025209 (2007).
- [25] J. Arnold, B. van den Brandt, M. Daum, Ph. Demierre, M. Finger, M. Finger, Jr., J. Franz, N. Goujon-Naef, P. Hautle, R. Hess, A. Janata, J. A. Konter, H. Lacker, C. Lechanoine-Leluc, F. Lehar, S. Mango, D. Rapin, E. Rösle, P. A. Schmelzbach, H. Schmitt, P. Sereni, M. Slunečka, A. Teglia, B. Vuaridel, Eur. Phys. J. C **17**, 83 (2000).
- [26] E. Hiyama, B. F. Gibson, and M. Kamimura, Phys. Rev. C **70**, 031001 (2004).